

## Supplemental Material

### Intratumoral T-cells have a Differential Impact on FDG-PET Parameters in Follicular Lymphoma

#### Supplemental Methods

FDG-PET parameters .....	2
Gene expression.....	2
TCR $\beta$ sequencing.....	3
Analysis of cellular glucose-uptake.....	4
Histopathology and flow cytometry of diagnostic tissue biopsies.....	4
Statistical Analysis.....	5
Supplementary References.....	5

#### Supplemental Tables

Supplemental Table S1. Correlative analysis between CD4 <sup>+</sup> , CD8 <sup>+</sup> and CD19 <sup>+</sup> cellular glucose uptake and SUV <sub>lesional</sub> . .....	6
Supplemental Table S2. Baseline pre-therapy FDG-PET parameters.....	7
Supplemental Table S3. Normalized <i>CD4</i> and <i>CD8A</i> gene expression in follicular lymphoma patients.....	9
Supplemental Table S4. Normalized <i>CD4</i> , <i>CD8A</i> , <i>CD19</i> and <i>CD68</i> gene expression and SUV <sub>lesional</sub> values from pre-biopsy FDG-PET scans .....	11
Supplemental Table S5. Flow-cytometry antibodies and fluorochromes used for fluorescence activated cell sorting (FACS) sorting of intratumoral T-cell subsets for TCR $\beta$ sequencing, and for analysis of cellular glucose-uptake .....	12

#### Supplemental Figures

Supplemental Figure S1. Consort diagram providing details of FDG-PET parameters, FL <i>de-novo</i> tumor tissue and sample testing performed.....	13
Supplemental Figure S2. Histological FL grade and serum lactate dehydrogenase (LDH) are not associated with pre-treatment TMTV.....	14

## Supplemental Methods

### FDG-PET parameters

Pre-treatment  $^{18}\text{F}$ -fluorodeoxyglucose-positron emission tomography-computed tomography (FDG-PET) data in digital imaging and communications (DICOM) format were obtained for functional parameter measurements. All FDG-PET scans were obtained from the same scanner.

Two independent reviewers computed maximum standardized uptake value ( $\text{SUV}_{\text{max}}$ ), total metabolic tumor volume (TMTV) and total lesional glycolysis (TLG) using a customized MIM software workflow (MIM Software Inc, OH, USA). Maximum standardized uptake value ( $\text{SUV}_{\text{max}}$ ) was defined as the single voxel with the highest uptake in a lesion. Individual lesions of interest were identified by visual assessment of FDG-PET images and thereafter TMTV was obtained by summing the metabolic volume of all lesions. TMTV was calculated using a (i)  $\text{SUV} \geq 41\%$  of lesional  $\text{SUV}_{\text{max}}$  method ( $41\% \text{SUV}_{\text{max}}$ ) as recommended by the European Association of Nuclear Medicine,<sup>1</sup> and (2) fixed  $\text{SUV} \geq 2.5$  threshold method ( $\text{SUV} \geq 2.5$ ), as previously described.<sup>2,3</sup> TLG is the sum of the MTVs (using 41%  $\text{SUV}_{\text{max}}$  method) of individual lesions multiplied by their average SUV.<sup>1</sup> The bone marrow was considered involved only if there was focal uptake, and the spleen was included if there was either focal uptake or diffuse uptake 150% higher than the background liver activity.<sup>4</sup>

Twelve patients had a pre-therapy FDG-PET scan performed *prior* to their diagnostic excisional node biopsy. Lesional  $\text{SUV}_{\text{max}}$  ( $\text{SUV}_{\text{lesional}}$ ) within the subsequently excised node was obtained, providing a direct measure of FDG avidity within the tissue biopsy. In these 12 patients, the median time interval between the FDG-PET scan and subsequent biopsy was 15 days (interquartile range, 5-38 days). And in the patients who had their excisional biopsy prior to their FDG-PET scan ( $n=51$ ), the median time interval between the biopsy and scan was 20 days (interquartile range, 8-29 days).

### Gene expression

In the Brisbane cohort, RNA was extracted from sequential scrolls of archival follicular lymphoma (FL) formalin-fixed paraffin embedded (FFPE) samples using the Qiagen AllPrep DNA/RNA FFPE Kit. T-cell immune infiltration was determined using a targeted NanoString (NanoString Technologies, USA) panel of 12 clinically pertinent immune effector ( $CD137$ ,  $CD4$ ,  $CD7$ ,  $CD8A$ ,  $TNF\alpha$ ), immune checkpoint ( $PD-1$ ,  $PD-L1$ ,  $PD-L2$ ,  $TIM3$ ,  $LAG3$ ,  $FOXP3$ )

and macrophage (*CD68*) molecules, as previously published.<sup>5</sup> Normalization genes used in this code-set were *GAPDH*, *OAZ1*, *PGAM1* and *PGK1*. For each sample, a standardized Z-score was computed from *CD4* and *CD8A* gene counts. The average *CD4*, *CD8A* Z-score was then used to categorize T-cell<sup>LO</sup> (quartile 1-3) and T-cell<sup>RICH</sup> (quartile 4) nodes. Normalized data is provided in **supplemental Table S3**.

In the twelve patients in whom a staging FDG-PET scan was performed prior to their diagnostic excisional node biopsy, the Maxwell RNA FFPE Kit was used for RNA extraction. The nCounter PanCancer immune profiling panel (730 immune related genes + 40 housekeeping genes, NanoString) was used to permit analysis of *CD4*, *CD8A*, *CD19* and *CD68* gene expression within the subsequently biopsied FL node. This allowed to test for an association between the FDG-PET derived SUV<sub>lesional</sub> status and *CD4*, *CD8A*, *CD19* and *CD68* gene expression from the same lesion. Normalized data is provided in the **supplemental Table S4**.

### TCR $\beta$ sequencing

Twenty-one fresh de-aggregated and immediately cryopreserved baseline FL tumor infiltrating lymphocytes (TILs) from the Brisbane cohort were used. Samples underwent fluorescence activated cell sorting (FACS) into phenotypically distinct intra-tumoral T-cell subsets: T-follicular helper cells (T<sub>FH</sub> cells; CXCR5<sup>+</sup>ICOS<sup>+</sup>CD4<sup>+</sup>), regulatory T-cells (T<sub>REG</sub>; CD25<sup>HI</sup>CD127<sup>LO</sup>CXCR5<sup>-ve</sup>CD4<sup>+</sup>), non-T<sub>FH</sub>/T<sub>REG</sub> CD4<sup>+</sup> T-cells and CD8<sup>+</sup> T-cells.<sup>6</sup> Of the 21 FL TILs, 14 underwent further CD8<sup>+</sup> cell sorting into distinct PD-1<sup>+</sup>LAG<sup>-ve</sup> (activated), PD-1<sup>+</sup>LAG3<sup>+</sup> (exhausted) and PD-1<sup>-ve</sup>LAG3<sup>-ve</sup> (resting) CD8<sup>+</sup> T-cells.<sup>7</sup> Flow-cytometry antibodies and fluorochromes are included in **supplemental Table S5**. Total genomic DNA was then extracted within these individual T-cell subsets in each patient using the QIAamp DNA Micro Kit (Qiagen). High-throughput, deep-resolution (3-6 replicates) next-generation sequencing (NGS) of the TCR $\beta$  gene was performed using the immunoSEQ hsTCR $\beta$  assay (Adaptive Biotechnologies), as previously described.<sup>8,9</sup> In brief, TCR $\beta$  CDR3 regions were amplified by a multiplex, bias-controlled PCR with a pool of primer pairs targeting *V* and *J* genes of T-cells, and subsequently tagged with unique barcoded primer pairs. Purified barcoded PCR products were sequenced on an Illumina NextSeq-500 analyzer. Following quality control review, the raw NGS data were uploaded onto the immunoSEQ pipeline and Simpson's clonality was calculated according to the equation:  $\sum_{i=1}^R P_i^2$  where R = total number of rearrangements; i = each rearrangement;  $P_i$  = productive frequency of rearrangement. The Simpson's clonality metric ranges from 0 to 1 where values approaching 0 represent a completely even sample, and 1 represents a monoclonal sample. 'All CD4<sup>+</sup> T-cell clonality was generated by merging

the individual DNA rearrangements from the 3 CD4<sup>+</sup> T-cells subsets, and subsequently calculating clonality.

T-cell clonality values within all sorted T-cell subsets was independent to, and not associated with the CD19<sup>+</sup> B-cell percentage within malignant nodes (as enumerated by flow cytometry).

### **Analysis of cellular glucose-uptake**

Eight FL TILs from the Brisbane cohort and 20 FL TILs from the Canberra cohort were used to assess cellular glucose-uptake within CD4<sup>+</sup> T-cells, CD8<sup>+</sup> T-cells and CD19<sup>+</sup> B-cells. Dimethyl sulphoxide (DMSO) was used as a cryoprotective agent to maintain cell viability of TILs.

The 2-NBDG glucose-uptake assay kit (Abcam) was used to determine cellular glucose-uptake.<sup>10</sup> The kit uses 2-NBDG, a fluorescently labelled deoxyglucose analogue. FL TILs were rapidly thawed and assayed for viability and a minimum of 200,000 live cells were required. Thereafter, cells were washed, resuspended in complete cell-growth medium (RPMI1640 + 1% sodium pyruvate + 1% penicillin-streptomycin-glutamine + 10% heat-inactivated FBS, Gibco) and rested at 37°C for 2 hours. Cells were then washed and rested glucose free RPMI1640 medium (Gibco) for 2 hours. After 2 hours of glucose starvation, 12.5µg/mL 2-NBDG was added to cells and incubated at 37°C for 1 hour, as determined by our in-house optimisation assay. After additional washes, cells were incubated with the surface antibody cocktail following manufacturer's instruction. The samples were analysed on FACSymphony A5 and data was analysed using Kaluza software (Beckman Coulter). Flow-cytometry antibodies and fluorochromes are included in **supplemental Table S5**.

### **Histopathology and flow cytometry of diagnostic tissue biopsies**

FL diagnostic histopathology reports (from excisional lymph node biopsies), which includes the FL histological grading, were obtained. Where available, H&E-stained tissue sections for Ki67 immunohistochemistry (IHC) were reviewed from the Brisbane cohort. In the 33 diagnostic biopsies that had Ki67 IHC, these were separated into a low Ki67 (<20%) and high Ki67 (≥20%) expression, as previously published.<sup>11</sup> Additionally, paired diagnostic tissue flow cytometry reports from the Brisbane cohort were obtained to assess infiltration by light-chain (kappa or lambda) restricted CD19<sup>+</sup> FL B-cells.<sup>12</sup> Flow cytometric analysis was performed on BDFACS Canto (BD Biosciences).

## Statistical Analysis

Comparisons of patient variables between groups used the Wilcoxon rank-sum test. *P* values <0.05 were statistically significant. Statistical analysis used Prism v7.03 (GraphPad Software, CA).

## Supplementary References

1. Boellaard R, Delgado-Bolton R, Oyen WJG, et al. FDG PET/CT: EANM procedure guidelines for tumour imaging: version 2.0. *European Journal of Nuclear Medicine and Molecular Imaging*. 2015;42(2):328-354.
2. Ilyas H, Mikhaeel NG, Dunn JT, et al. Defining the optimal method for measuring baseline metabolic tumour volume in diffuse large B cell lymphoma. *European journal of nuclear medicine and molecular imaging*. 2018;45(7):1142-1154.
3. Barrington SF, Trotman J, Sahin D, et al. Baseline PET-Derived Metabolic Tumor Volume Metrics Did Not Predict Outcomes in Follicular Lymphoma Patients Treated with First-Line Immunochemotherapy and Antibody Maintenance in the Phase III GALLIUM Study. *Blood*. 2018;132(Suppl 1):2882-2882.
4. Meignan M, Cottreau AS, Versari A, et al. Baseline Metabolic Tumor Volume Predicts Outcome in High-Tumor-Burden Follicular Lymphoma: A Pooled Analysis of Three Multicenter Studies. *J Clin Oncol*. 2016;34(30):3618-3626.
5. Tobin JWD, Keane C, Gunawardana J, et al. Progression of Disease Within 24 Months in Follicular Lymphoma Is Associated With Reduced Intratumoral Immune Infiltration. *J Clin Oncol*. 2019;JCO1802365.
6. Yang Z-Z, Kim HJ, Wu H, et al. TIGIT Expression Is Associated with T-cell Suppression and Exhaustion and Predicts Clinical Outcome and Anti-PD-1 Response in Follicular Lymphoma. *Clinical Cancer Research*. 2020;26(19):5217.
7. Yang ZZ, Kim HJ, Villasboas JC, et al. Expression of LAG-3 defines exhaustion of intratumoral PD-1(+) T cells and correlates with poor outcome in follicular lymphoma. *Oncotarget*. 2017;8(37):61425-61439.
8. Robins HS, Campregher PV, Srivastava SK, et al. Comprehensive assessment of T-cell receptor beta-chain diversity in alphabeta T cells. *Blood*. 2009;114(19):4099-4107.
9. Keane C, Gould C, Jones K, et al. The T-cell Receptor Repertoire Influences the Tumor Microenvironment and Is Associated with Survival in Aggressive B-cell Lymphoma. *Clin Cancer Res*. 2017;23(7):1820-1828.
10. Zou C, Wang Y, Shen Z. 2-NBDG as a fluorescent indicator for direct glucose uptake measurement. *J Biochem Biophys Methods*. 2005;64(3):207-215.
11. Ad K, Hedwig AT, John MMR, et al. The prognostic significance of the intra-follicular tumor cell proliferative rate in follicular lymphoma. *Haematologica*. 2007;92(2):184-190.
12. Keane C, Gill D, Vari F, Cross D, Griffiths L, Gandhi M. CD4+ Tumor infiltrating lymphocytes are prognostic and independent of R-IPI in patients with DLBCL receiving R-CHOP chemotherapy. *American Journal of Hematology*. 2013;88(4):273-276.

**Supplemental Table S1.** Correlative analysis between CD4<sup>+</sup>, CD8<sup>+</sup> and CD19<sup>+</sup> cellular glucose uptake and SUV<sub>lesional</sub>.

<b>CELL SUBSET</b>	<b>Pearson r</b>	<b>P-value</b>
<b>CD4<sup>+</sup></b>	0.70	0.054
<b>CD8<sup>+</sup></b>	0.44	0.280
<b>CD19<sup>+</sup></b>	0.55	0.156

**Supplemental Table S2.** Baseline pre-therapy FDG-PET parameters

<b>FL No.</b>	<b>TMTV, cm<sup>3</sup> (41%<i>SUV</i><sub>max</sub>)</b>	<b>TMTV, cm<sup>3</sup> (<i>SUV</i> ≥ 2.5)</b>	<b>Highest <i>SUV</i><sub>max</sub></b>	<b>TLG, g</b>
1	451.03	680.56	23.44	5384.28
2	14.41	14.47	6.25	63.48
3	18.69	33.33	23.23	140.98
4	29.43	43.47	6.86	37.84
5	247.73	282.26	12.07	1616.95
6	32.31	33.06	3.22	64.16
7	602.68	1731.89	37.36	10107.12
8	2518.82	2691.83	7.41	8033.26
9	701.46	1108.4	8.98	2485.95
10	942.04	1080.66	11.1	4711.43
11	268.35	484.98	21.62	3569.1
12	824.02	1724.09	7.7	3539.68
13	108.74	111.07	6.11	252.8
14	384.33	485.68	11.45	1339.22
15	619.69	1636.85	16.26	5155.21
16	21.87	33.67	13	165.85
17	65.44	83.5	9.06	312.11
18	627.42	748.94	8.59	2906.68
19	73.07	154	9.76	293.13
20	262.22	943.63	15.89	2069.32
21	10.04	12	7.31	42.15
22	166.87	1437.59	23.4	1280.65
23	1810.78	2297.94	8.18	7424.03
24	1097.8	1603.98	10.27	5863.26
25	283.15	575.97	20.41	2550.06
26	142.55	148.66	4.2	242.7
27	465.46	1740.19	14.46	1553.06
28	42.98	51.57	14.81	90.96
29	18.58	19.23	4.14	38.01
30	86.52	101.37	11.63	346.97
31	59.99	70.92	5.14	146.49
32	6.57	6.57	3.84	20.92
33	487.78	747.33	9.47	2292.45
34	110.39	127.84	7.98	449.94
35	1465.85	1841.61	25.72	7583.15
36	218.57	266.84	7.9	1034.26
37	430.24	523.01	5.66	1298.15
38	1830.67	3172.58	11.3	9005.98
39	1642.9	3426.23	10.54	8712.75
40	232.11	1130.26	18.14	1799.4

FL No.	TMTV, cm <sup>3</sup> (41% $SUV_{max}$ )	TMTV, cm <sup>3</sup> ( $SUV \geq 2.5$ )	Highest $SUV_{max}$	TLG, g
41	29.61	38	8.97	169.54
42	75.51	79.69	6.02	272.88
43	16.3	24.25	8.09	75.6
44	16.39	18.50	7.39	70.93
45	208.78	277.12	5.93	609.04
46	154.27	436.72	9.53	483.22
47	17.47	21.97	6.49	26.91
48	23.16	25.42	4.93	62.01
49	2527.58	4442.49	10.67	11319.99
50	994.82	1476.06	9.6	2878.34
51	25.88	26.12	6.65	59.74
52	32.66	34.73	8.45	146.27
53	11.64	13.5	4.33	29.1
54	650.75	1550.72	25.39	5028.63
55	98.14	115.22	6.61	242.12
56	44.62	46.99	5.89	139.31
57	48.19	78.01	7.93	209.8
58	751.68	1531.51	17.29	4118.98
59	268.29	402.52	8.71	1040.16
60	709.38	921.97	10.18	2715.33
61	295.16	825.55	13.49	1683.79
62	1416.92	2409.98	8.13	4848.69
63	447.21	886.68	9.36	1585.87

**Abbreviations:** TMTV, total metabolic tumor volume;  $SUV_{max}$ , maximum standardized uptake value; TLG, total lesion glycolysis



**Supplemental Table S3.** Normalized *CD4* and *CD8A* gene expression in follicular lymphoma patients

FL No.	Age	Sex	Stage	FLIPI	<i>CD4</i>	<i>CD8A</i>
1	49.8	M	4	2	1528.26	1582.12
2	72.4	M	1	2	3472.18	1134.68
3	77.4	M	1	1	1579.91	1297.89
4	51.7	F	3	2	3281.32	1701.83
5	58.2	F	4	3	2152.18	2654.36
6	45.9	M	1	2	2122.14	1055.99
7	45.6	F	4	3	2273.92	2052.49
8	69.2	M	4	3	1149.73	619.84
9	73.9	F	3	3	560.4	311.44
10	30.5	F	4	3	1233.21	1706.84
11	46.2	F	2	2	1589.21	1412.41
12	56.1	M	4	1	2189.49	2137.71
13	71.1	M	4	3	3600.68	7135.29
14	68.8	F	4	3	186.65	191.7
15	64.0	F	4	3	1321.24	3312.78
16	56.6	F	4	2	1726.45	1915.33
17	67.1	M	4	3	2200.14	3433.24
18	49.8	F	4	2	1614.59	1606.15
19	60.9	F	3	3	2127.28	2279.96
20	83.4	F	3	3	2022.32	2135.45
21	56.0	M	2	1	775.54	895.75
22	29.2	M	3	1	1922.19	1201.93
23	44.9	M	4	3	2474.09	1201.41
24	58.4	F	3	1	165.89	180.97
25	54.5	F	3	3	1630.82	1444.77
26	51.3	F	4	3	1388.36	1227.68
27	60.2	F	3	3	507.79	546.5
28	71.9	F	2	1	3627.21	3990.09
29	50.6	F	3	2	2436.68	3897.52
30	68.4	F	3	3	816.74	533.64
31	43.0	F	2	1	2583.63	7567
32	83.5	F	1	1	822.56	1821.76
33	52.9	F	4	3	1492.58	4265.08
34	52.5	F	4	2	2390.24	3145.72
35	56.9	M	4	2	1304.4	1576.55
36	62.9	M	4	3	1944.46	864.16
37	69.6	F	4	3	3347.28	493.08
38	65.4	M	4	3	955.84	1106.61
39	52.4	M	4	2	2668.71	1093.49
40	53.2	F	4	2	1541.19	1076.71

<b>FL No.</b>	<b>Age</b>	<b>Sex</b>	<b>Stage</b>	<b>FLIPI</b>	<b>CD4</b>	<b>CD8A</b>
<b>41</b>	61.0	M	3	2	2527.18	854.12
<b>42</b>	81.7	F	4	3	3385.49	1698.71
<b>43</b>	63.3	M	3	2	3067.06	1086.67
<b>44</b>	68.8	F	3	2	3368.61	601.2
<b>45</b>	76.9	M	3	3	2670.34	6226.68

**Supplemental Table S4.** Normalized *CD4*, *CD8A*, *CD19* and *CD68* gene expression and  $SUV_{lesional}$  values from pre-biopsy FDG-PET scans

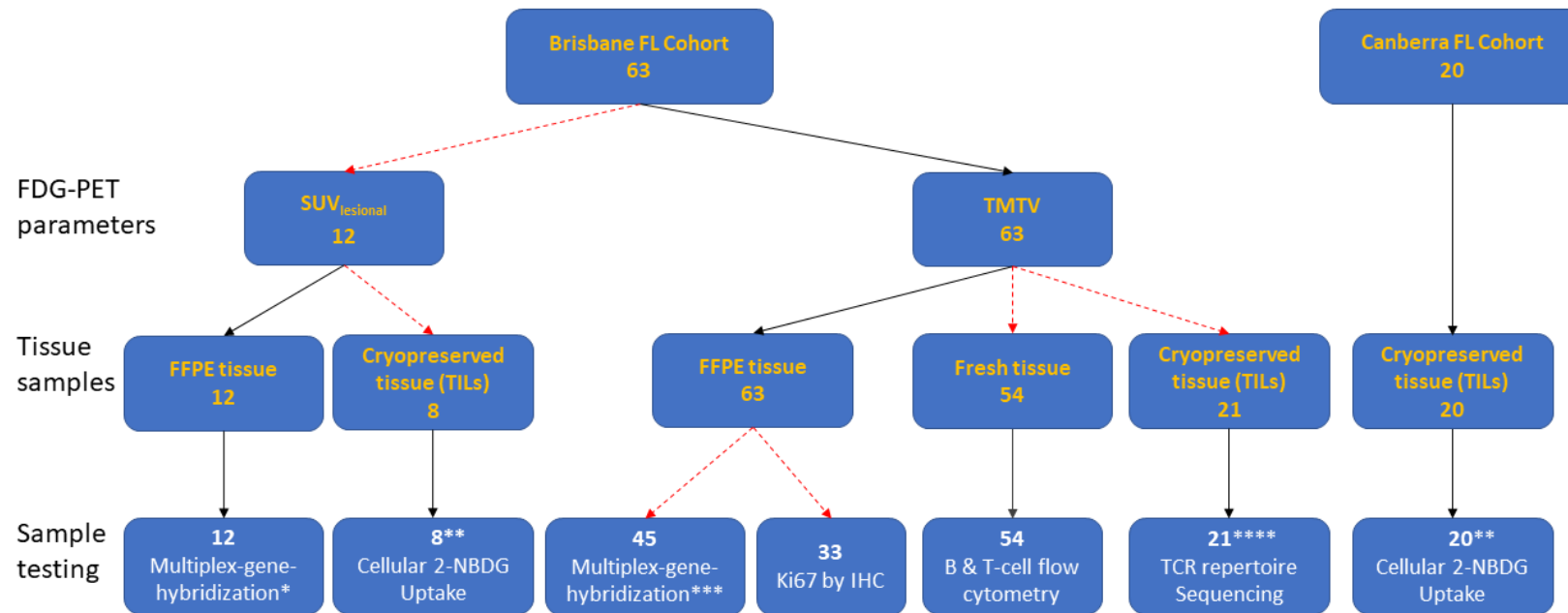
<b>FL No.</b>	<b>Age</b>	<b>Sex</b>	<b>Stage</b>	<b>FLIPI</b>	<b><i>CD4</i></b>	<b><i>CD8A</i></b>	<b><i>CD68</i></b>	<b><i>CD19</i></b>	<b><math>SUV_{lesional}</math></b>
14	69	F	4	3	298.48	85.77	253.88	20	3.54
21	56	M	2	1	838.91	513.01	421.31	2643.12	6.53
25	55	F	3	3	751.4	296.15	357.58	3367.9	8.15
48	72	F	4	2	361.52	241.93	333.92	982.45	4.78
51	40	F	3	2	433.44	495.14	277.65	1261.77	6.65
52	70	F	1	1	777.70	672.51	451.49	696.15	7.54
53	78	F	2	2	360.22	321.57	234.22	779.20	4.33
55	72	F	3	2	569.49	229.04	578.86	1154.59	5.24
56	40	M	4	2	358.82	212.63	242.76	759.28	5.89
57	71	M	4	3	696.36	653.82	709.57	1009.61	7.93
58	67	F	4	5	665.79	900.71	455.23	741.82	7.97
60	75	M	4	2	465.96	335.8	436.43	962.55	8.99

**Abbreviations:**  $SUV_{lesional}$ , lesional  $SUV_{max}$

**Supplemental Table S5.** Flow-cytometry antibodies and fluorochromes used for fluorescence activated cell sorting (FACS) sorting of intratumoral T-cell subsets for TCR $\beta$  sequencing, and for analysis of cellular glucose-uptake

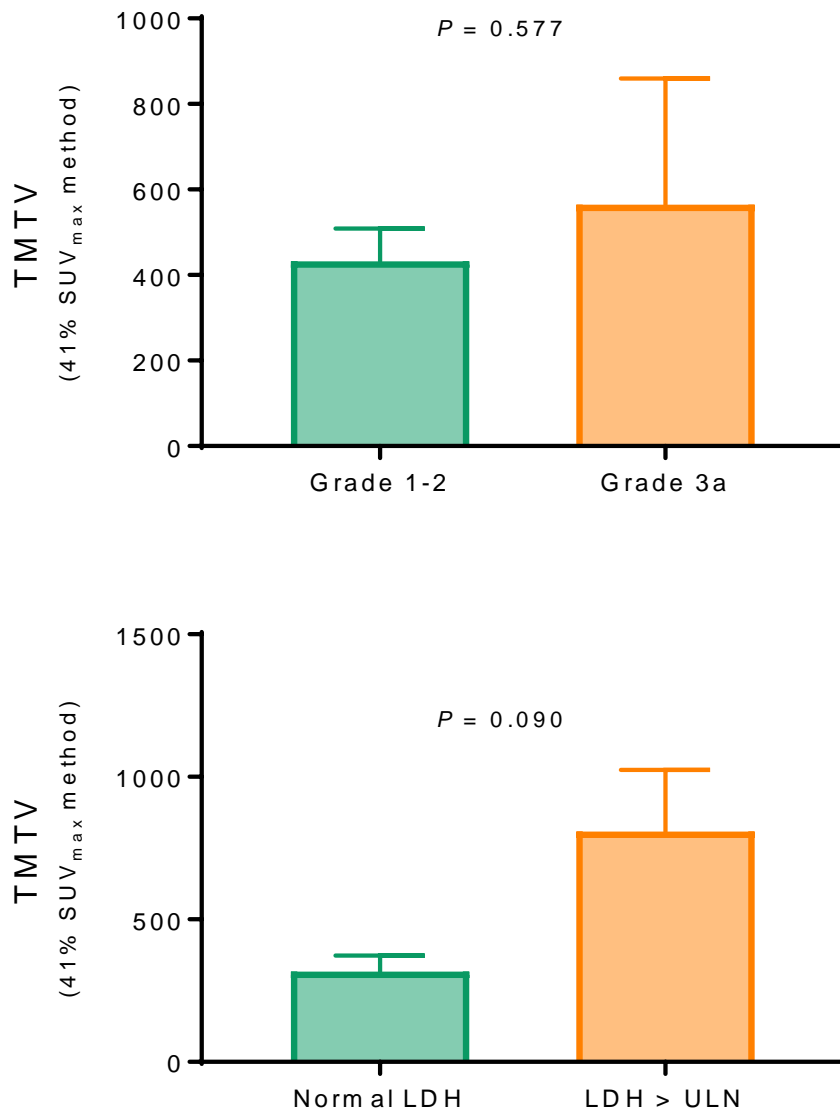
Marker	Fluorochrome	Clone	Isotype	Manufacturer
<b>Different T-cell subsets panel</b>				
CD11c	FITC	B-ly6	Mouse IgG1, $\kappa$	BD Biosciences
CD14	FITC	M $\phi$ P9	Mouse IgG2b, $\kappa$	BD Biosciences
CD16	FITC	3G8	Mouse IgG1, $\kappa$	Biolegend
CD19	FITC	H1B19	Mouse IgG1, $\kappa$	BD Biosciences
ICOS	PE	DX29	Mouse IgG1, $\kappa$	BD Biosciences
CD127	PerCP/Cy5.5	hIL-7R-M21	Mouse IgG1, $\kappa$	BD Biosciences
CD25	APC	BC96	Mouse IgG1, $\kappa$	Biolegend
CXCR5	BV421	J252D4	Mouse IgG1, $\kappa$	Biolegend
CD8	BV785	SK1	Mouse IgG1, $\kappa$	Biolegend
CD3	BUV395	SK7	Mouse IgG1, $\kappa$	BD Biosciences
CD4	BUV737	SK3	Mouse IgG1, $\kappa$	BD Biosciences
Live/dead fixable green dead cell stain	488 nm	-	-	Invitrogen
<b>CD8 subsets panel</b>				
CD11c	FITC	B-ly6	Mouse IgG1, $\kappa$	BD Biosciences
CD14	FITC	M $\phi$ P9	Mouse IgG2b, $\kappa$	BD Biosciences
CD16	FITC	3G8	Mouse IgG1, $\kappa$	Biolegend
CD19	FITC	H1B19	Mouse IgG1, $\kappa$	BD Biosciences
CD3	APC	UCHT1	Mouse IgG1, $\kappa$	BD Pharmingen
CD8	BV785	SK1	Mouse IgG1, $\kappa$	Biolegend
PD-1	PE	PD1.3.1.3	Mouse IgG2b, $\kappa$	Miltenyi Biotec
LAG3	BUV395	T45-530	Mouse IgG1, $\kappa$	BD Biosciences
Live/dead fixable green dead cell stain	488 nm	-	-	Invitrogen
<b>2-NBDG panel</b>				
CD11c	PE/Cy5	B-ly6	Mouse IgG1, $\kappa$	BD Biosciences
CD14	AF700	M5E2	Mouse IgG2a, $\kappa$	BD Biosciences
CD16	PE/Cy5	3G8	Mouse IgG1, $\kappa$	BD Biosciences
CD19	PE/Cy7	SJ25C1	Mouse IgG1, $\kappa$	BD Biosciences
CD3	BUV496	UCHT1	Mouse IgG1, $\kappa$	BD Biosciences
CD4	BUV805	SK3	Mouse IgG1, $\kappa$	BD Biosciences
CD8	BUV563	RPA-T8	Mouse IgG1, $\kappa$	BD Biosciences
Fixable viability stain 700	640 nm	-	-	BD Biosciences
2-NBDG	488 nm	-	-	Abcam

**Supplemental Figure S1.** Consort diagram providing details of FDG-PET parameters, FL *de-novo* tumor tissue and sample testing performed.



Brisbane FL Cohort from the Princess Alexandra Hospital; Canberra FL Cohort from the Canberra Hospital. \*Multiplex-gene-hybridization (NanoString) was performed to permit analysis of *CD4*, *CD8A*, *CD19* and *CD68* gene expression. \*\*8 FL TILs from the Brisbane Cohort and 20 FL TILs from the Canberra cohort underwent cellular 2-NBDG assessment within  $CD19^+$ ,  $CD8^+$  and  $CD4^+$  cell subsets. \*\*\*Multiplex-gene-hybridization (NanoString) was performed to determine intra-tumoral T-cell states ( $T\text{-cell}^{LO}$  vs.  $T\text{-cell}^{RICH}$ ). \*\*\*\*Twenty-one FL TILs underwent TCR repertoire sequencing within FACS sorted  $CD4^+$   $T_{FH}$ ,  $T_{REG}$ , Non- $T_{FH}/T_{REG}$  cells and  $CD8^+$  T-cells. Of these 21 FL TILs, 14 underwent further TCR repertoire sequencing within sorted  $PD1^+LAG3^{-ve}$ ,  $PD1^+LAG3^+$  and  $PD1^{-ve}LAG3^{-ve}$   $CD8^+$  T-cells. Abbreviations: FL: follicular lymphoma;  $SUV_{lesional}$ : lesional  $SUV_{max}$ ; TMTV: total metabolic tumor volume; FFPE: formalin-fixed paraffin embedded; TILs: tumor infiltrating lymphocytes; IHC: immunohistochemistry; TCR: T-cell receptor.

**Supplemental Figure S2.** Histological FL grade and serum lactate dehydrogenase (LDH) are not associated with pre-treatment TMTV



TMTV (cm<sup>3</sup>) was determined by the 41%SUV<sub>max</sub> method. Grade 1-2 ( $n = 55$ ) and Grade 3 ( $n = 8$ ); Normal LDH ( $n = 46$ ) and LDH > upper limit of normal (ULN,  $n = 17$ ).